The Three-Dimensional Structure of the Human Pi Class Glutathione Transferase P1-1 in Complex with the Inhibitor Ethacrynic Acid and Its Glutathione Conjugate[†,‡]

Aaron J. Oakley,[§] Jamie Rossjohn,[§] Mario Lo Bello,[||] Anna Maria Caccuri,[||] Giorgio Federici,[||] and Michael W. Parker*[,§]

The Ian Potter Foundation Protein Crystallography Laboratory, St. Vincent's Institute of Medical Research, 41 Victoria Parade, Fitzroy, Victoria 3065, Australia, and Department of Biology, University of Rome "Tor Vergata", Via della Ricerca Scientifica, 00133 Rome, Italy

Received September 13, 1996[⊗]

ABSTRACT: The potent diuretic drug ethacrynic acid has been tested in clinical trials as an adjuvant in chemotherapy. Its target is the detoxifying enzyme glutathione transferase which is often found overexpressed in cancer tissues. We have solved the crystal structures of human pi class glutathione transferase P1-1 in complex with the inhibitor ethacrynic acid and its glutathione conjugate. Ethacrynic acid is found to bind in a nonproductive mode to one of the ligand binding sites of the enzyme (the H site) while the glutathione binding site (G site) is occupied by solvent molecules. There are no structural rearrangements of the G site in the absence of ligand. The structure indicates that bound glutathione is required for ethacrynic acid to dock into the H site in a productive binding mode. The binding of the ethacrynic acid−glutathione conjugate shows that the contacts of the glutathione moiety with the protein are identical to those observed in crystal structures of the enzyme with other glutathione-based substrates and inhibitors. The ethacrynic acid moiety of the conjugate binds in the H site in a fashion that has not been observed in crystal structures of other glutathione-based inhibitor complexes. The crystal structures implicate Tyr 108 as an electrophilic participant in the Michael addition of glutathione to ethacrynic acid.

Mammalian cells express a diverse range of enzymes that metabolize toxins for eventual elimination from the host. In the first step, hydrophobic toxins (xenobiotics) are converted to more reactive species by enzymes such as cytochrome P-450. The product can then be enzymatically inactivated by chemical conjugation with various groups, rendering the toxins more water-soluble and less toxic for eventual elimination via the urinary tract. The archetypical enzyme family in the latter step are the glutathione S-transferases (GSTs,[1] EC 2.5.1.18). The GSTs are a family of enzymes that conjugate electrophilic substrates to the tripeptide glutathione (GSH, γ-Glu-Cys-Gly). Mammalian cytosolic GSTs exist either as homodimers or as heterodimers with a subunit molecular mass of about 25 kDa and with one active site per monomer [for a review, see Wilce and Parker (1994)]. They can be classified into four distinct families (alpha, mu, pi, and theta) based on studies of substrate specificity and primary structures (Mannervik et al., 1985; Meyer et al., 1991). The amino acid sequence identities between any two members within a class is typically greater than 70% whereas the figure is typically about 30% between classes. GSTs have at least two ligand binding sites per monomer; the G site is very specific for glutathione whereas the binding site for the xenobiotic substrate (H site) is less specific in keeping with the ability of GSTs to react with a wide variety of toxic agents. A further binding site has recently been characterized based on the crystal structure of *Schistosoma japonica* GST complexed to the antischistosomal drug praziquantel (McTigue et al., 1995). The binding site, referred to as either the "ligandin" or the "nonsubstrate" binding site, is located in the dimer interface and is thought to be the site of binding of large molecules including heme and bile salts.

GSTs have been implicated in the development of resistance of tumors toward various anti-cancer drugs [for reviews, see Coles and Ketterer (1990), Waxman, (1990), Tsuchida and Sato (1992), and Hayes and Pulford, (1995)]. A number of human tumors, including cancers of the colon, stomach, pancreas, uterine cervix, breast, and lung as well as lymphoma and melanoma, have been shown to express raised levels of pi class GST (Coles & Ketterer, 1990; Tsuchida & Sato, 1992, and references cited therein). Several investigators have noted increased levels of pi class GST in a variety of tumor cell lines that are resistant to a range of anti-cancer drugs including chlorambucil (Wang & Tew, 1985; Yang et al., 1992), nitrogen mustards (Buller et al., 1987), adriamycin (Batist et al., 1986), doxorubicin (Batist et al., 1986), mitomycin C (Taylor et al., 1985), melphalan (Gupta et al., 1989), *cis*-DDP (Teichner et al., 1987), and hepsulfam (Armstrong et al., 1992). Furthermore,

[†] Financial support from the Anti-Cancer Council of Victoria and the National Research Council ACRO is gratefully acknowledged. A.J.O. is a recipient of a National Health & Medical Research Council Postgraduate Research Scholarship, J.R. is a recipient of a Royal Society Fellowship, and M.W.P. is a Wellcome Australian Senior Research Fellow.

[‡] The crystallographic coordinates have been deposited in the Brookhaven Protein Data Bank under the filenames 2GSS and 3GSS.

* Address correspondence to this author.

[§] St. Vincent's Institute of Medical Research.

[||] University of Rome "Tor Vergata".

[⊗] Abstract published in *Advance ACS Abstracts,* December 15, 1996.

[1] Abbreviations: CDNB, 1-chloro-2,4-dinitrobenzene; DTT, 1,4-dithiothreitol; EA, ethacrynic acid; EA−GSH, glutathione conjugate of ethacrynic acid; EDTA, ethylenediamine tetraacetic acid; GSH, glutathione; GST, glutathione *S*-transferase; MES, 2-(*N*-morpholino)-ethanesulfonic acid; NCS, noncrystallographic symmetry.

S0006-2960(96)02316-1 CCC: $14.00

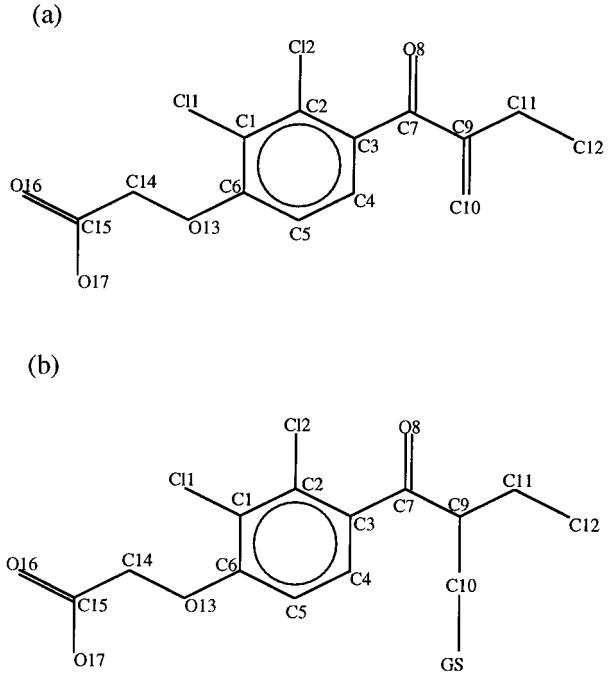

FIGURE 1: Schematic representation of (a) EA and (b) EA−GSH. The numbering scheme is taken from Lamotte et al. (1978).

expression of several recombinant GSTs in cultured cell lines confers resistance toward anti-cancer drugs (Puchalski & Fahl, 1990; Black et al., 1990). GST-dependent conjugates of the anti-cancer drugs hepsulfam (Armstrong et al., 1992), melphalan (Dulik et al., 1986), and chlorambucil (Pallante et al., 1986) have been demonstrated.

The diuretic drug ethacrynic acid ([2,3-dichloro-4-(2-methylenebutyryl)phenoxy]acetic acid, see Figure 1a) is an inhibitor of alpha, mu, and pi class GSTs (Ploemen et al., 1990). A number of investigators have explored the possibility of inhibiting GSTs with ethacrynic acid (EA) as a means of overcoming acquired multidrug resistance. The toxicity of chlorambucil in resistant cells could be significantly increased by use of ethacrynic acid (Yang et al., 1992), and the inhibitor sensitizes human leukemia, lymphoma, and myeloma cells toward nitrogen mustards and doxorubicin (Nagourney et al., 1989). Inhibition of pi class GST P1-1 with ethacrynic acid has also produced a 2-fold increase in the cytotoxic effect of melphalan on human melanoma cells (Hansson et al., 1991). In a recent study, ethacrynic acid was administered in conjunction with an ethylene imine (thiotepa) to 27 previously treated patients with advanced cancer (O'Dwyer et al., 1991). Pi class GST activity was reduced, and the tumors were found to have increased sensitivity to thiotepa. However, ethacrynic acid was found to cause extreme diuresis, hyperglycemia, hypocalcemia, and hypomagnesemia. These side effects have proved too severe to continue on with Phase II trials of the inhibitor. Despite the potential benefits of GST inhibitors and despite the large number of GST inhibitors that have been synthesized to date, very few compounds have proved suitable for clinical trials.

We recently solved the crystal structure of human pi class GST P1-1 in complex with the inhibitor *S*-hexyl-GSH (Reinemer et al., 1992, and unpublished results). Here we present the structure of the enyzme in the presence of the inhibitors ethacrynic acid and its glutathione conjugate. The structure of the human alpha class enzyme complexed to these inhibitors has recently been presented (Cameron et al., 1995). Our results define the key residues in binding and conjugation of ethacrynic acid to glutathione in the pi class enzyme and provide an explanation as to why the conjugation reaction is much more efficient in this isoenzyme compared to the alpha class isoenzyme.

Table 1: Crystallographic Data for the Glutathione Transferase Inhibitor Complexes

data	EA complex	EA−GSH complex
space group	*C2*	*C2*
cell dimensions		
a,b,c (Å)	77.5, 90.0, 68.9	77.7, 89.4, 68.6
β (deg)	97.7	97.4
max resolution (Å)	1.9	1.9
no. of crystals	1	1
total no. of observations	93866	61022
no. of unique reflections	36158	33121
completeness of data (%)[a]	98.0 (96.4)	90.7 (87.3)
no. of data $>3\sigma_I$ (%)[a]	71.7 (36.6)	63.4 (30.8)
I/σ_I	11.4 (3.0)	8.7 (2.6)
multiplicity	2.6 (2.3)	1.8 (1.7)
R_{merge} (%)[a]	8.4 (27.5)	8.8 (27.1)

[a] The values in parentheses are for the highest resolution bin (1.97 Å − 1.90 Å).

EXPERIMENTAL PROCEDURES

Crystallization and Data Collection. Crystallization was performed by the hanging-drop vapor diffusion method (McPherson, 1982) using 24-well tissue culture plates. A 2 μL droplet of an 8 mg/mL protein solution containing 10 mM phosphate buffer (pH 7.0), 1 mM EDTA and 2 mM mercaptoethanol was mixed with an equal volume of reservoir solution. The reservoir solution consisted of 23−27% (w/v) ammonium sulfate, 55 to 65 mM DTT, and 0.1 M MES buffer (pH range 5.4−5.8). The drop was applied to a siliconized coverslip which was sealed to the top of the well with vacuum grease. Each well contained 1 mL of reservoir solution. The trials were carried out at a constant temperature of 22 °C. The drops were allowed to equilibrate for 1−2 days before they were streak-seeded with a cat's whisker from drops containing crystals grown under similar conditions. Crystals appeared in the shape of thick plates within 1 day after seeding and grew to maximal dimensions of 0.2 mm × 0.9 mm × 0.5 mm. For EA, a small amount of solid was placed in the drop 1 day prior to data collection. For EA−GSH, a small amount of solid was placed in the drop at regular intervals over a 7 day period prior to data collection. The EA was obtained from Sigma Chemical Co. (St. Louis, MO), and EA−GSH was synthesized according to Ploemen et al. (1990).

The X-ray diffraction data were collected using a MAR-RESEARCH area detector with CuK_α X-rays generated by a Rigaku RU-200 rotating-anode X-ray generator. Both complexes were collected at 100 K using an Oxford Cryosystems Cryostream Cooler. Prior to flash-freezing, the crystals were transferred to artificial mother liquor containing 20% glycerol. The diffraction data were processed and analyzed using programs in the HKL (Otwinowski, 1993) and CCP4 suites (1994). The relevant data statistics are presented in Table 1.

Structure Solution and Refinement. The initial analysis of the inhibitor complexes included examination of difference Fourier maps calculated with SIGMAA-weighted $F_{inhibitor}$ −

Table 2: Refinement Statistics for the Glutathione Transferase Inhibitor Complexes

	EA complex	EA−GSH complex
non-hydrogen atoms	3262 protein	3262 protein
	38 inhibitor	78 inhibitor
	323 water	360 water
	5 sufate	5 sulfate
	36 MES buffer	24 MES buffer
resolution (Å)	15.0−1.9	15.0−1.9
$R_{conventional}$ (%)	21.0	20.6
R_{free} (%)	23.0	23.4
reflections used in $R_{conventional}$ calculations		
number, completeness (%)	34661, 91.1	31475, 86.2
rmsds from ideal geometry		
bonds (Å)	0.007	0.007
angles (deg)	1.3	1.3
dihedrals (deg)	22.1	22.3
impropers (deg)	1.3	1.2
residues in most favorable regions of Ramachandran plot (%)	92.7	94.1

F_{native} and $2F_{inhibitor} - F_{native}$ coefficients (Read, 1986) where native amplitudes and phases were calculated from the final GST model in complex with *S*-hexyl-GSH (Reinemer et al., 1992, and unpublished results). The $2F_{inhibitor} - F_{native}$ electron density map was further improved by 10 cycles of 2-fold noncrystallographic averaging using MAMA (Kleywegt & Jones, 1994), RAVE (Kleywegt & Jones, 1994), and CCP4 (1994) program suites. Refinement began with the final *S*-hexyl-GSH complex model (Reinemer et al., 1992, and unpublished results) which had the *S*-hexyl-GSH inhibitor and water molecules removed. Rigid-body refinement in XPLOR version 3.1 (Brünger et al., 1987) was used to compensate for any possible changes in crystal packing. As the asymmetric unit of the crystal contained two GST monomers, use was made of the noncrystallographic symmetry restraints on all non-hydrogen atoms throughout the course of refinement of both inhibitors. For the EA model, bond lengths and angles were derived from the crystal structure of the molecule determined by Lamotte and coworkers (Lamotte et al., 1978). For the EA−GSH conjugate, bond lengths and angles were derived from a model built and energy-minimized using programs in the BIOSYM software suite (BIOSYM Technologies Inc., San Diego, CA). The final refinement statistics of both models are presented in Table 2.

The starting model for the EA complex, the refined *S*-hexyl-GSH complex model observed in the C2 space group (*R*-factor = 20.0% and R_{free} = 24.5% for resolution limits 6.0−1.95 Å; unpublished results) after removal of inhibitor molecules, gave an *R*-factor of 38.8% (R_{free} = 38.4%) which reduced to 33.9% (R_{free} = 33.2%) after rigid-body refinement. Maps generated from this model revealed clear and interpretable density in the H site. After two rounds of positional refinement followed by individual *B*-factor refinement with tight NCS restraints, the *R*-factor reduced to 25.0% (R_{free} = 27.3%). At this stage, the ethacrynic acid molecule was built into the model and included in the refinement. The fitting of the molecule into the electron density was unambiguous (Figure 2a,b). The complex was finally subjected to a round of positional refinement which included NCS-restrained individual *B*-factor refinement giving a final *R*-factor of 24.5% (R_{free} = 26.2%). Attempts to weaken the NCS restraints resulted in increases of the R_{free} value and hence were not pursued. The average temperature factor for the EA molecule at this stage was 34.6 Å^2 compared with a value of 22.9 Å^2 for the protein atoms. The higher temperature factors recorded here for the inhibitor and in other studies of GST−inhibitor complexes (Cameron et al., 1995; Ji et al., 1995) could be attributable to partial occupancy of the inhibitor. A low occupancy could partly reflect the poor solubility of EA in aqueous solution. After application of a bulk solvent correction, the final *R*-factor was 21.0% (R_{free} = 23.0%) for all data between 15.0 and 1.9 Å resolution. The estimated average error in atomic coordinates from a Luzzati plot is between 0.2 and 0.3 Å (data not shown). The fit of the inhibitor to the final electron density maps is shown in Figure 2a,b.

For the EA−GSH conjugate complex, the refined *S*-hexyl-GSH complex model as observed in the *C2* space group (unpublished results) was used as the starting model. The *S*-hexyl-GSH inhibitor of the *S*-hexyl-GSH complex model was omitted prior to use. The starting model gave an *R*-factor of 34.7% (R_{free} = 34.8%) which reduced to 33.2% (R_{free} = 33.5%) after rigid-body refinement. The model was then subjected to two cycles of positional and isotropically-restrained individual *B*-factor refinement with inclusion of water and MES buffer molecules (*R*-factor = 25.0%, R_{free} = 27.2%). The averaged electron density maps calculated from this model allowed unambiguous placement of the inhibitor. The density for the chlorine atoms of the inhibitor was very clear. If the atoms at the chlorine positions were given scattering factors for carbon in the Fourier calculations, two strong peaks greater than 6σ were positioned over both atoms, confirming the identification of the chlorine atoms. After two more rounds of refinement and rebuilding, the model yielded an *R*-factor of 22.9% (R_{free} = 25.4%). After application of a bulk solvent correction, the final *R*-factor was 20.6% (R_{free} = 23.4%) for all data between 15.0 and 1.9 Å resolution. The estimated average error in atomic coordinates from a Luzzati plot was between 0.2 and 0.3 Å (data not shown). The fit of the inhibitor to the final electron density maps is shown in Figure 2c,d.

A stereochemical analysis of the refined structures with the program PROCHECK (Laskowski et al., 1993) gave values either similar or better than expected for structures refined at similar resolutions.

RESULTS

Ethacrynic Acid Complex. EA binds in the H site site of the enzyme in a similar position to that found for the hexyl moiety of the *S*-hexyl-GSH complex crystal structure (Reinemer et al., 1992) (Figure 3). The inhibitor sits in a hydrophobic pocket lined with the side chains of Tyr 7, Phe 8, Pro 9, and Val 10 and the aliphatic portions of Arg 13, Val 35, Ile 104, and Tyr 108. The ring moiety of the inhibitor is stacked between the aromatic side chains of Phe 8 and Tyr 108 (Figures 3 and 4). The two chlorine atoms are nestled in a pocket formed by Phe 8, Val 10, and Tyr 108. The butyryl group is nestled in a shallow hydrophobic pocket on the surface of the protein made up of residues Phe 8, Val 35, and Trp 38. The ketone moiety points out toward solvent and does not form any contacts with the protein. A solvent molecule is within hydrogen bonding distance of this group. The carboxylic acid moiety of the inhibitor forms a hydrogen bond to the Nϵ atom of Arg 13

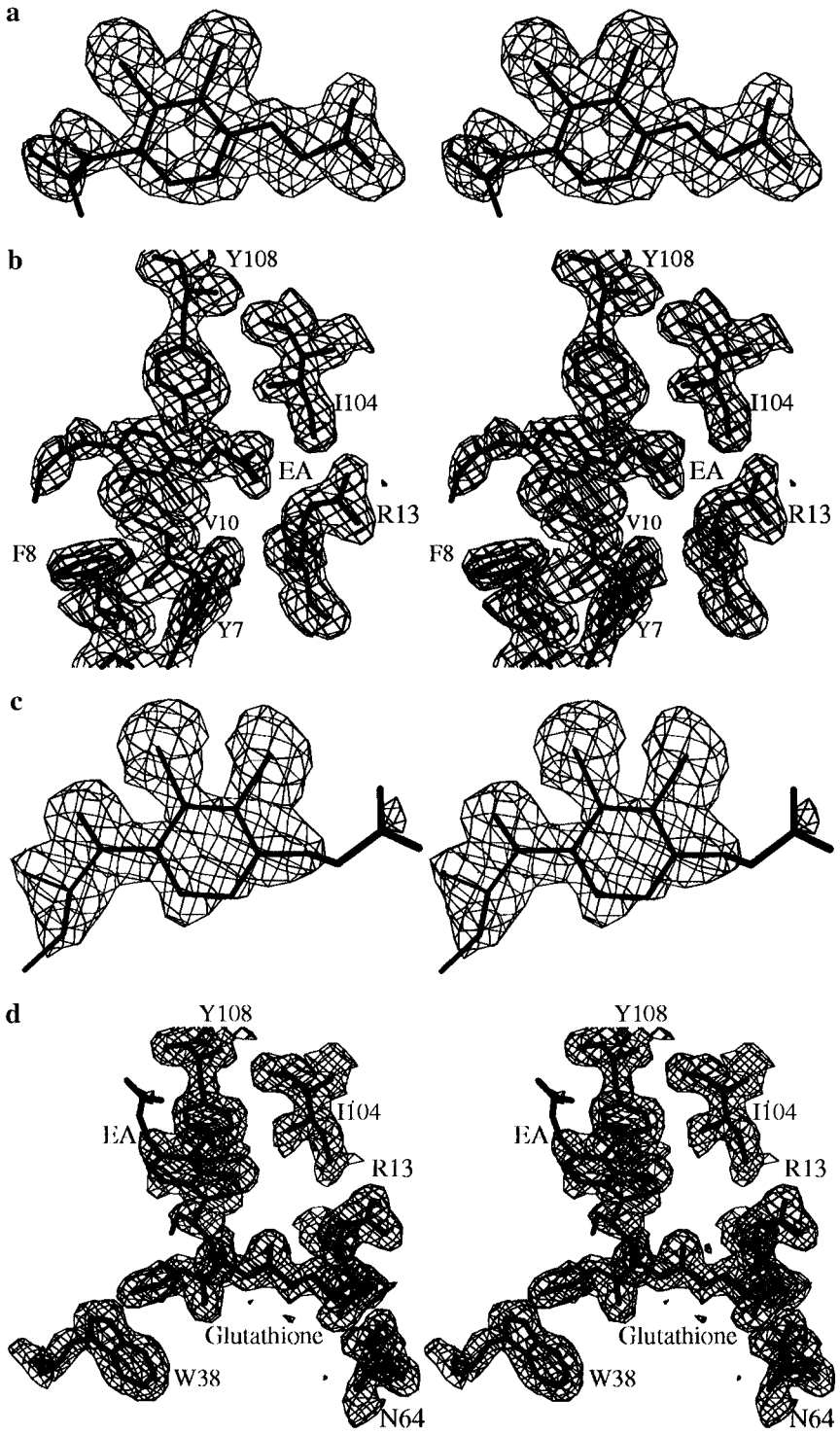

FIGURE 2: Stereo diagram of the final $2F_{inhibitor} - F_{calc}$ electron density maps of the complexes in the vicinity of the inhibitor binding site of human GST P1-1. All maps were calculated using all reflections between 15.0 and 1.9 Å and contoured at the 1σ level. (a) Density for the inhibitor in the EA complex. (b) Density of the inhibitor and surrounding side chains in the EA complex. (c) Density for the EA moiety in the EA−GSH complex. (d) Density of the inhibitor and surrounding side chains in the EA−GSH complex.

and a water-mediated interaction with Tyr 7. In total, there are 38 van der Waals contacts (<4 Å), 2 protein−inhibitor hydrogen bonds, and 3 water-mediated protein−inhibitor hydrogen bonds (Figure 4). There was no significant electron density observed in the G site with the exception of two spherical blobs that have been interpreted as water molecules. A superposition of the EA complex on the *S*-hexyl-GSH complex structure indicates no significant movement of side chains (Figure 3). The root-mean-square deviation in α-carbon positions is 0.2 Å with no movements greater than 0.8 Å.

Despite the absence of ligand in the G site, there are no structural changes in the main-chain or side-chain atoms that line the G site. However, low-resolution (2.8 Å) structures of the EA complex and of two apo-GST structures, all of which were based on X-ray diffraction data collected at room temperature, demonstrate a dramatically increased mobility in helix 2 and its flanking regions (unpublished results). Helix

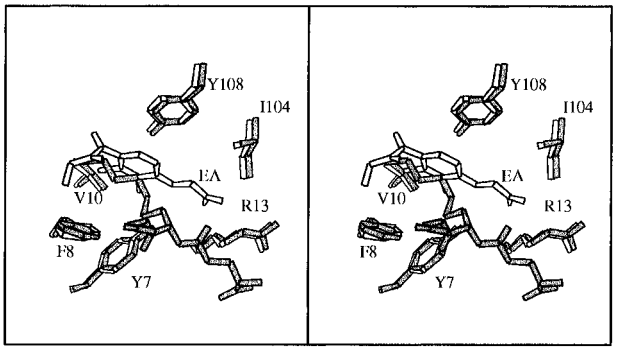

FIGURE 3: Superposition of *S*-hexyl-GSH and EA complex structures in the vicinity of the active site. Filled bonds are for the *S*-hexyl-GSH complex structure; hollow bonds are for the inhibitor complex. The figure was generated with the program MOLSCRIPT (Kraulis, 1991).

2 provides some of the residues that line the G site. Presumably, the low temperature used to collect the EA data set reported here has prohibited the increased flexibility of this region from being observed.

Ethacrynic Acid−Glutathione Conjugate Complex. The conjugation of GSH with EA can theoretically result in two possible diastereomers. After appropriate rotation of torsion angles so that each diastereomer would fit the electron density, the only significant difference between the two molecules is the positioning of the C9 and C11 atoms of the alkyl group (see Figures 1 and 5). The difference in positioning of these atoms is less than 0.6 Å and is not distinguishable in our electron density maps. We have chosen only one diastereomer for simplicity. Surprisingly, the aromatic ring of the inhibitor sits in a very different position than that of the hexyl moiety in the *S*-hexyl-GSH complex structure (Figure 5) (Reinemer et al., 1992), although the ethyl group of EA does superimpose on the hexyl moiety of the latter complex. The carboxylate moiety of EA points out toward solution and does not make any protein contacts (Figures 5 and 6). One chlorine atom nestles against Ile 104 while the other points out to solution. The EA ketone moiety is within hydrogen-bonding distance (3.2 Å) of the hydroxyl of Tyr 108, but the two groups lie parallel to one another. A water-mediated hydrogen bond between the two groups yields a much more convincing hydrogen-bonding geometry. In addition, there is a water-mediated bond between the ketone moiety and the side chain of Asn 204. The glutathione moiety of the inhibitor makes essentially identical contacts to residues in the G site of the enzyme as was observed with inhibitor *S*-hexyl-GSH (Reinemer et al., 1992). In total, there are 113 van der Waals interactions (<4 Å), 18 potential hydrogen-bonding interactions, 3 salt-bridging interactions, and 7 water-mediated contacts between protein and inhibitor. As was the case for the EA complex, superposition of the EA−GSH complex on the (*C2* space group) *S*-hexyl-GSH complex structure indicates no significant movement of side chains in the active site (Figure 5). The root-mean-square deviation in α-carbon positions is 0.1 Å, with no deviations greater than 0.5 Å.

Comparison of the EA and EA−GSH Complexes. The EA moieties of each complex bind in completely different positions and orientations, although both are located in the H site of the enzyme (Figure 7). The aromatic rings do lie in the same plane but sit adjacent to one another with a shift of 2.5 Å, and the rings have rotated 120° to each other with respect to the positioning of the chlorine atoms. The aromatic ring of the EA−GSH complex packs directly under the ring of Tyr 108 in a parallel stacking interaction while the aromatic ring of the EA complex sits at a less optimum angle so as to optimize packing contributions from the rings of both Tyr 108 and Phe 8. We have superimposed all the available pi class crystal structures which have GSH conjugates bound. These include the human enzyme in complex with *S*-hexyl-GSH (Reinemer et al., 1992) and the mouse enzyme in complex with *S*-hexyl-GSH and *S*-(*p*-nitrobenzyl)-GSH (García-Sáez et al., 1994). The results demonstrate that the aromatic ring of the EA complex binds in a similar position to the other inhibitors. The aromatic rings of EA and the nitrobenzyl inhibitor almost superimpose with the ring of the latter inhibitor slightly rotated so as to optimize its parallel stacking with Phe 8. Thus, athough the aromatic rings of EA, EA−GSH, and *S*-(*p*-nitrobenzyl)-GSH are all stacked between the rings of Tyr 108 and Phe 8, subtle variations in the positioning and orientation of each inhibitor result in optimization of the interaction with either of the two protein side chains or a compromise between the two.

Other important differences between the EA and EA−GSH complexes concern interactions of the carboxylate and ketone moieties. In the EA complex, the carboxylate forms an important interaction with an arginine residue (Figure 4) whereas in the EA−GSH complex it does not interact with the protein at all (Figure 6). There is some precedence for the latter finding with no interaction observed between the protein and the nitro group of the mouse GST inhibitor (García-Sáez et al., 1994). The ketone moiety of EA does not contact the protein in the EA complex (Figure 4) but is involved in water-mediated contacts in the EA−GSH complex (Figure 6).

Despite these differences, there are some similarities between the EA and EA−GSH complexes. The chlorine and butyryl (or ethyl in the conjugate) groups pack against hydrophobic surfaces in both complexes. There is no significant movement of side chains within a 15 Å sphere of the active site between the two complexes. The α-carbon atoms of the EA and EA−GSH complex models superimpose with an rms deviation of 0.2 Å with only two deviations greater than 0.5 Å [Pro 2 (0.9 Å) and Asn 110 (0.5 Å)].

Comparisons to the Alpha Class GST Complexes. It is not straightforward to directly compare the structures of the pi class GST complexes to those of the alpha class enzyme. Although they share the same overall canonical GST fold, the pairwise amino acid sequence identity is only 32% (Sinning et al., 1993). In particular, the H sites are very different due to an additional helix at the C-terminal end of the alpha enzyme which forms part of the H site wall. Nevertheless, some qualitative comparisons can be made.

A surprising result of both studies has been the orientation of the EA molecule in the H site (Cameron et al., 1995). Rather than expose the carboxylate moiety to solvent and burying the butyryl group into the hydrophobic regions of the G site, the EA inhibitor has bound so that the carboxylate forms hydrogen-bonding interactions to G site arginine residues in each enzyme. This results in the formation of a nonproductive complex with respect to GSH conjugation. Superposition of the alpha and pi class structures shows that the aromatic rings of EA sit adjacent and orthogonal to each other. It would not be possible for each inhibitor to adopt the positioning of the other in the opposing enzyme because

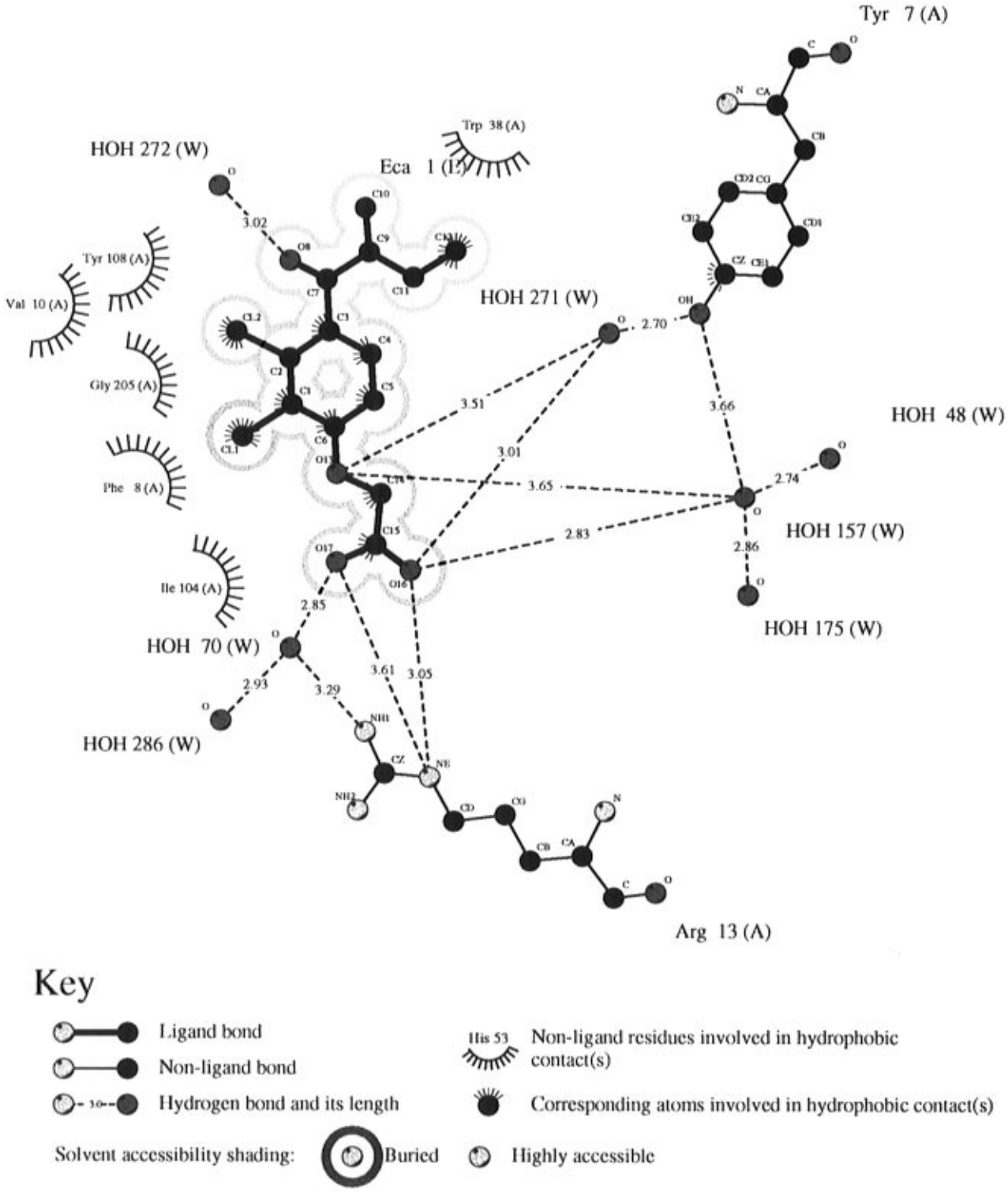

FIGURE 4: Schematic drawing of residues and solvent molecules that interact with EA. This figure was produced using the program LIGPLOT (Wallace et al., 1995).

of steric clashes. However, there are further common features between the two complexes besides the arginine interaction. The aromatic rings of EA stack in parallel fashion against aromatic side chains of the two enzymes (Tyr 108 and Phe 8 in the pi class GST and Phe 222 in the alpha class GST), and the chlorine atoms nestle in hydrophobic pockets.

The binding of EA−GSH in both classes of GST is similar to the extent that the GSH moiety binds to equivalent residues and that EA is bound in the H site. In addition, the aromatic rings of the EA moiety stack against aromatic side chains of the each enyzme. However, there a number of important differences. The aromatic rings of the EA moiety sit orthogonal to each other upon superposition, and the orientation could not be exchanged between enzymes without the creation of steric clashes. The carbonyl oxygen O8 hydrogen bonds to Tyr 9 in the alpha class GST whereas it bonds to Tyr 108 and Asn 204 via a water molecule in the pi class enzyme. The EA carboxylate hydrogen bonds to a main-chain amino nitrogen and two water molecules in the alpha class enzyme whereas there are no protein contacts with the pi class enzyme. We observe only one conformation of the

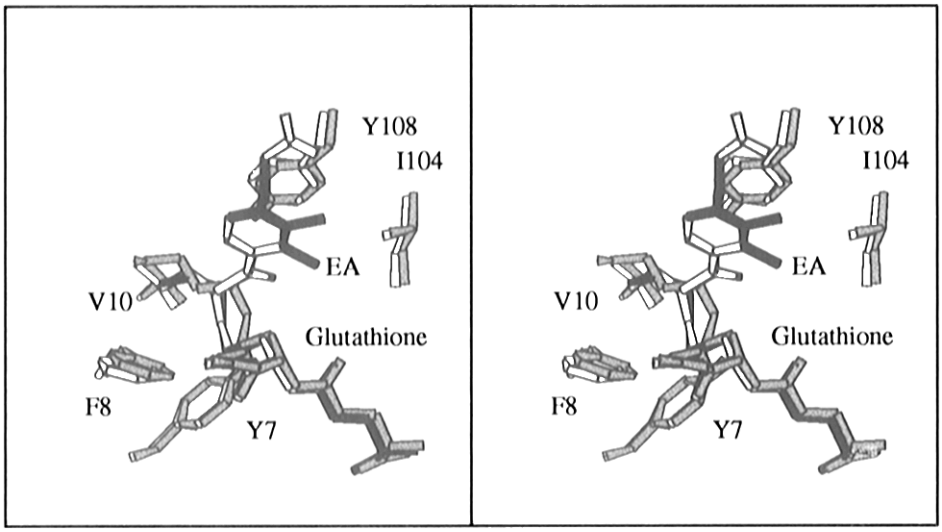

FIGURE 5: Superposition of *S*-hexyl-GSH and EA−GSH complex structures in the vicinity of the active site. Filled gray bonds are for the *S*-hexyl-GSH complex structure, the unfilled bonds represent the EA−GSH complex structure, and the solid black bonds are the alternative diastereomer of EA−GSH. The figure was generated with the program MOLSCRIPT (Kraulis, 1991).

inhibitor, unlike the observed binding of EA−GSH to the alpha class enzyme (Cameron et al., 1995). [In the alpha class enzyme, two conformations were observed in which there was an approximately 140° rotation of the dichlorophenoxy group about the axis defined by the substituents off the C3 and C6 positions of the ring (Figure 1b).]

DISCUSSION

EA is a known inhibitor of GSTs but in addition can act as a substrate. EA is thought to form a conjugate with GSH via Michael addition, both spontaneously and by GST-driven catalysis (Ploemen et al., 1990; Phillips & Mantle, 1991; Awasthi et al., 1993). The α,β-unsaturated ketone moiety is the target for conjugation by GSH (Awasthi et al., 1993). The alpha, mu, and pi class enzymes are known to catalyze the reaction, with the pi class enzyme the most efficient (Ploemen et al., 1990). The reaction of the pi class GST with EA is often considered a characteristic feature of this isoenzyme (Mannervik & Danielson, 1988). The EA−GSH conjugate also acts as an inhibitor. In the case of human pi class GST, the EA−GSH conjugate is a more potent inhibitor than the parent compound (K_i = 1.5 vs 11.5 μM, respectively) (Awasthi et al., 1993).

The kinetic work on the pi class enzyme found in the literature is often contradictory. Some groups have reported that EA and its conjugate act as reversible inhibitors and inhibition of the enzyme by EA is competitive toward the model substrate 1-chloro-2,4-dinitrobenzene (CDNB) but noncompetitive toward GSH (Ploemen et al., 1990; Phillips & Mantle, 1991). Other workers claim that EA is noncompetitive with either substrate (Awasthi et al., 1993). Our results support the former finding because EA is observed to bind in the H site, the binding site for CDNB, but does not encroach on the G site where GSH binds. Ploemen and co-workers (Ploemen et al., 1990) found EA is a more potent inhibitor of the pi class enzyme than the EA−GSH conjugate while Awasthi and co-workers (Awasthi et al., 1993) found the opposite. Our results demonstrate that there are considerably more contacts of EA−GSH with the protein than its parent compound, and hence we would support the results of the latter group.

One group have described an allosteric binding site for EA which increases the V_{max} of the reaction between CDNB and GSH (Phillips & Mantle, 1991). There is some evidence that EA can react irreversibly with the pi class enzyme and the site of reaction is the cysteine at position 47 (Ploemen et al., 1993a; Phillips & Mantle, 1993). Although this cysteine in the human enzyme is highly reactive (Lo Bello et al., 1990; Desideri et al., 1991), we saw no signs of covalent modifications to this residue in our crystal structures. It is likely that the high levels of DTT used in the crystallization trails did not favor this reaction. In addition, as EA is only sparingly soluble under our crystallization conditions, it is possible that the retro-Michael addition is favored so there is very little conjugate with cysteine 47 formed (Ploemen et al., 1994b). The possible inactivation of the enzyme by EA suggests the order of addition of reactants in any kinetic analysis is important and may explain some of the anomalous results in the literature.

The nonproductive binding of EA in the pi class enzyme was unexpected. In order for the Michael addition between EA and GSH to proceed, the EA molecule must somehow reorientate itself in the H site. It seems very likely that bound GSH is responsible for causing the binding of EA in a productive mode. The inhibitor could not bind to the GSH-bound enzyme in the orientation observed in the EA complex because of van der Waals repulsions between the inhibitor carboxylate tail and GSH. Under physiological conditions, the concentration of GSH in normal cells (1−10 mM) would ensure the large majority of enzyme molecules would be bound to GSH, and thus productive binding of the inhibitor would be ensured.

Michael additions normally involve the nucleophilic attack on the β-alkene carbon of α,β-unsaturated carbonyl compounds. Our structural results provide a rationale for why the pi class enzyme is good at catalyzing the conjugation of EA to GSH. The reactivity of the nucleophile, GSH, is enhanced by Tyr 7 which acts to stabilize the thiolate anion of the substrate [reviewed in Wilce and Parker (1994)]. In our EA−GSH structure, the electrophilicity of the EA β-alkene carbon is enhanced by the hydrogen bonding of Tyr 108 and Asn 204 via a water molecule to the EA ketone

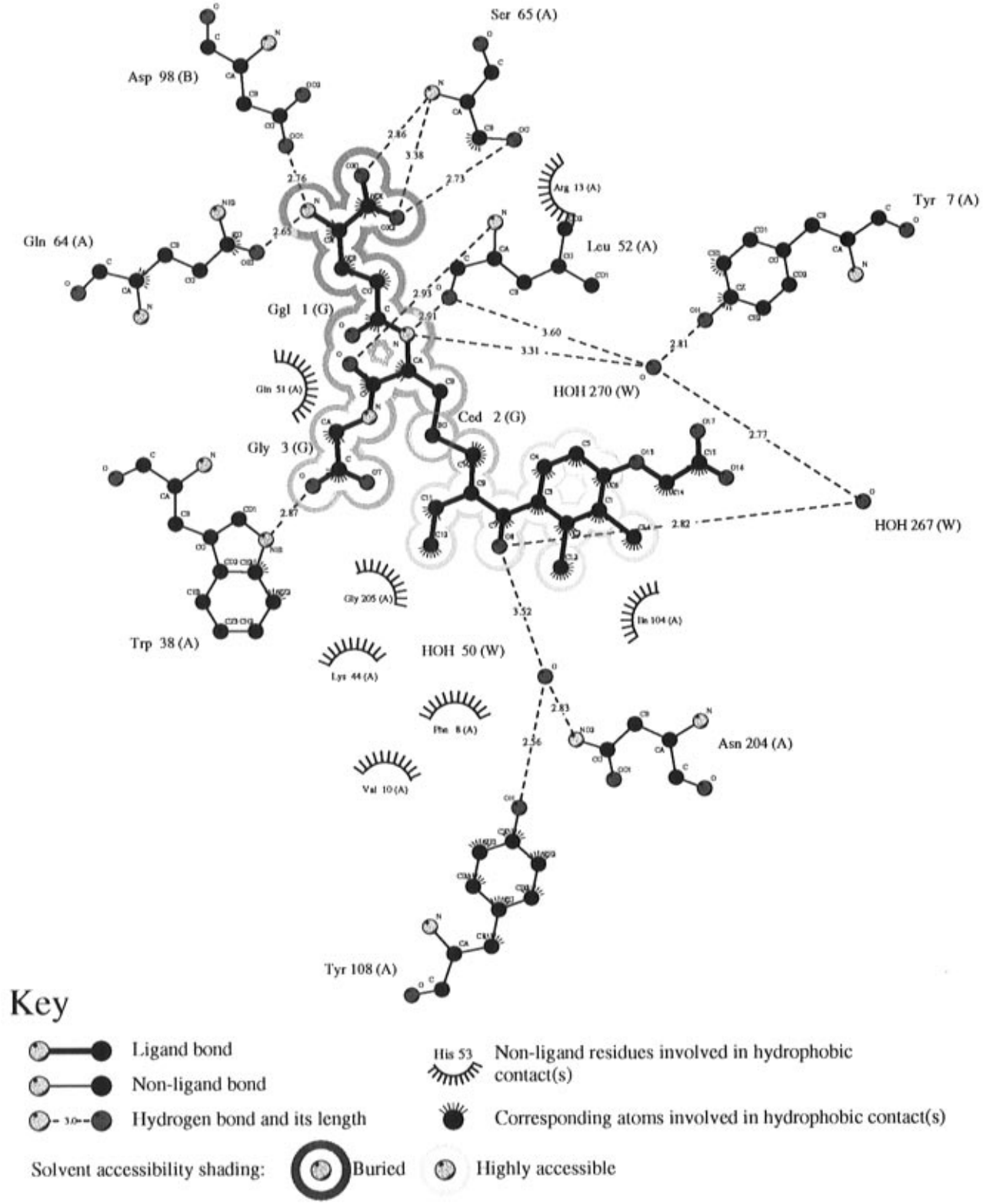

FIGURE 6: Schematic drawing of residues that interact with EA−GSH. Water-mediated interactions with the GSH moiety have been omitted for clarity. This figure was produced using the program LIGPLOT (Wallace et al., 1995).

oxygen (O8 in Figure 1). It is conceivable for a direct hydrogen-bonding interaction between the ketone oxygen and Tyr 108 by small changes in the orientation of the Tyr 108 side chain and the inhibitor. This is not the case for Asn 204, which is 6.0 Å distant of the ketone oxygen. Modeling of EA bound in a productive mode to the enzyme suggests a direct hydrogen-bonding interaction (distance of 3.4 Å) between Tyr 108 and the ketone oxygen is also possible. Movements of both the inhibitor and the side chain of Tyr 108 during the reaction mechanism could further enhance the interaction between the two. Our results suggest that the hydroxyl group of Tyr 108 contributes to the catalytic mechanism as a general acid in the Michael addition of glutathione to ethacrynic acid (Figure 8). Preliminary kinetic experiments with a Y108F mutant support a role for this residue in the catalysis of EA (M. Lo Bello, A. J. Oakley,

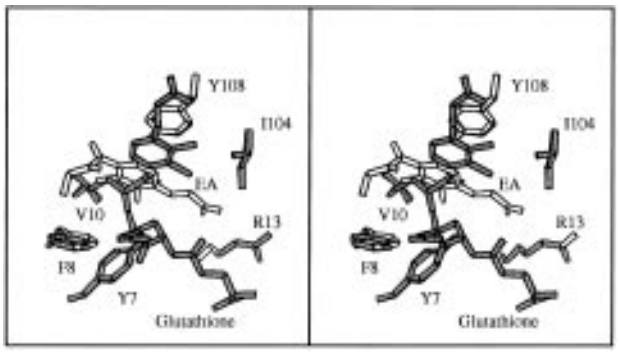

FIGURE 7: Superposition of EA and EA−GSH complex structures in the vicinity of the active site. Filled bonds are for the EA−GSH structure; hollow bonds are for the EA complex. The figure was generated with the program MOLSCRIPT (Kraulis, 1991).

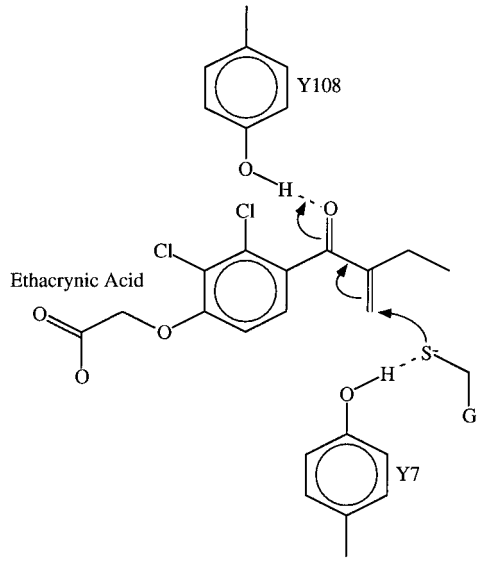

FIGURE 8: Possible mechanism for electrophilic assistance of Tyr 108 in the Michael addition of glutathione to ethacrynic acid.

A. Battistoni, A. P. Mazzetti, M. Nuccetelli, G. Mazzarese, J. Rossjohn, M. W. Parker, and G. Ricci, unpublished results).

The possible role of a tyrosine in the C-terminal domain in xenobiotic substrate binding and catalysis was first suggested for the mu class enzyme (Katusz & Colman, 1991; Barycki & Colman, 1993; Johnson et al., 1993; Ploemen et al., 1994a). In a sigma class GST from squid, there is a phenylalanine in the equivalent position, and the enzyme is not very efficient at Michael additions. Mutation of this residue to a tyrosine led to greatly improved activity (Ji et al., 1995). In the human alpha class enzyme, the equivalent tyrosine is replaced by a valine (Board & Webb, 1987). The low specific activity of the human alpha class enzyme for EA (Mannervik & Danielson, 1988; Ploemen et al., 1993b) could be explained by the absence of the tyrosine.

Our results form the basis for a structure-based design approach to identify inhibitors that maybe used as adjuvants in chemotherapeutic treatments using EA and EA−GSH as lead compounds.

ACKNOWLEDGMENT

We thank Kim, Larnie, and Boris Wilson for their sacrifices that made this work possible. We thank Matthew Wilce for his help in the early stages of this work.

REFERENCES

Armstrong, D. K., Gordon, G. B., Hilton, J., Streeper, R. T., Colvin, O. M., & Davidson, N. E. (1992) *Cancer Res. 52*, 1416−1421.
Awasthi, S., Srivastava, S. K., Ahmad, F., Ahmad, H., & Ansari, G. A. S. (1993) *Biochim. Biophys. Acta 1164*, 173−178.
Barycki, J. J., & Colman, R. F. (1993) *Biochemistry 32*, 13002−13011.
Batist, G., Tulpule, A., Sinha, B. K., Katki, A. G., Meyers, C. E., & Cowan, K. H. (1986) *J. Biol. Chem. 261*, 15544−15549.
Black, S. M., Beggs, J. D., Hayes, J. D., Bartszek, A., Muramatsu, M., Sakai, M., & Wolf, C. R. (1990) *Biochem. J. 268*, 309−315.
Board, P. G., & Webb, G. C. (1987) *Proc. Natl. Acad. Sci. U.S.A. 84*, 2377−2381.
Brünger, A. T., Kuriyan, J., & Karplus, M. (1987) *Science 235*, 458−460.
Buller, A. L., Clapper, M. L., & Tew, K. D. (1987) *Mol. Pharmacol. 31*, 575−578.
Cameron, A. D., Sinning, I., L'Hermite, G., Olin, B., Board, P. G., Mannervik, B. & Jones, T. A. (1995) *Structure 3*, 717−727.
Coles, B., & Ketterer, B. (1990) *CRC Crit. Rev. Biochem. Mol. Biol. 25*, 47−70.
CCP4 Suite (1994). *Acta Crystallogr. D50*, 750−763.
Desideri, A., Caccuri, A. M., Polizio, F., Bastoni, R., & Federici, G. (1991) *J. Biol. Chem. 266*, 2063−2066.
Dulik, D. M., Fenselau, C., & Hilton, J. (1986) *Biochem. Pharmacol. 35*, 3405−3409.
García-Sáez, I., Párraga, A., Phillips, M. F., Mantle, T. J., & Coll, M. (1994) *J. Mol. Biol. 237*, 298−314.
Gupta, V., Singh, S. V., Ahmad, H., Medh, R. D., & Awasthi, Y. C. (1989) *Biochem. Pharmacol. 38*, 1993−2000.
Hansson, J., Berhane, K., Castro, V. M., Jungnelius, U., Mannervik, B., & Ringborg, U. (1991) *Cancer Res. 51*, 94−98.
Hayes, J. D., & Pulford, D. J. (1995) *Crit. Rev. Biochem. Mol. Biol. 30*, 445−600.
Ji, X., von Rosenvinge, E. C., Johnson, W. W., Tomarev, S. I., Piatigorsky, J., Armstrong, R. N., & Gilliland, G. (1995) *Biochemistry 34*, 5317−5328.
Johnson, W. W., Liu, S., Ji, X., Gilliland, G. L., & Armstrong, R. N. (1993) *J. Biol. Chem. 268*, 11508−11511.
Katusz, R. M., & Colman, R. F. (1991) *Biochemistry 30*, 11230−11238.
Kleywegt, G., & Jones T. A. (1994) in *From First Map to Final Model* (Bailey, S., Hubbard, R., & Waller, D., Eds.) pp 59−66, EPSRC, Daresbury Laboratory, Warrington, U.K.
Kraulis, P. (1991) *J. Appl. Crystallogr. 24*, 946−950.
Lamotte, P. J., Campsteyn, H., Dupont, L., & Vermeire, M. (1978) *Acta Crystallogr. B34*, 2636−2638.
Laskowski, R. A., McArthur, M. W., Moss, D. S., & Thorton, J. M. (1993) *J. Appl. Crystallogr. 26*, 282−291.
Lo Bello, M., Retruzzelli, R., De Stefano, E., Tenedini, C., Barra, D., & Federici, G. (1990) *FEBS Lett. 263*, 389−391.
Mannervik, B., & Danielson, U. H. (1988) *CRC Crit. Rev. Biochem. 23*, 283−337.
Mannervik, B., Ålin, P., Guthenberg, C., Jensson, H., Tahir, M. K., Warholm, M., & Jornvall, H. (1985) *Proc. Natl. Acad. Sci. U.S.A. 82*, 7202−7206.
McPherson, A. (1982) *The Preparation and Analysis of Protein Crystals*, Wiley, New York.
McTigue, M. A., Williams, D. R., & Tainer, J. A. (1995) *J. Mol. Biol. 246*, 21−27.
Meyer, D. J., Coles, B., Pemble, S. E., Gilmore, K. S., Fraser, G. M., & Ketterer, B. (1991) *Biochem. J. 274*, 409−414.
Nagourney, R. A., Messenger, J. C., Kern, D. H., & Weisenthal, L. M. (1989) *Proc. Am. Assoc. Cancer Res. 30*, 574−580.
O'Dwyer, P. J., LaCreta, F., Nash, S., Tinsley, P. W., Schilder, R., Clapper, M. L., Tew, K. D., Panting, L., Litwin, S., Comis, R. L., & Ozols, R. F. (1991) *Cancer Res. 51*, 6059−6065.
Otwinowski, Z. (1993) in *Data Collection and Processing* (Sawyer, L., Isaacs, N., & Bailey, S., Eds.) pp 56−62, SERC Daresbury Laboratory, Warrington, U.K.
Pallante, S. L., Lisek, C. A., Dulik, D. M., & Fenselau, C. (1986) *Drug Metab. Dispos. 14*, 313−318.
Parker, M. W., Lo Bello, M., & Federici, G. (1990) *J. Mol. Biol. 213*, 221−222.

Phillips, M. F., & Mantle, T. J. (1991) *Biochem. J. 275*, 703−709.
Phillips, M. F., & Mantle, T. J. (1993) *Biochem. J. 294*, 57−62.
Ploemen, J. H. T. M., van Ommen, B., & van Bladeren, P. J. (1990) *Biochem. Pharmacol. 40*, 1631−1635.
Ploemen, J. H. T. M., Bogaards, J. J. P., Veldink, G. A., van Ommen, B., Jansen, D. H. M., & van Bladeren, P. J. (1993a) *Biochem. Pharmacol. 45*, 633−639.
Ploemen, J. H. T. M., van Ommen, B., Bogaards, J. J. P., & van Bladeren, P. J. (1993b) *Xenobiotica 23*, 913−923.
Ploemen, J. H. T. M., Johnson, W. W., Jespersen, S., Vanderwall, D., van Ommen, B., van der Greef, J., van Bladeren, P. J., & Armstrong, R. N. (1994a) *J. Biol. Chem. 269*, 26890−26897.
Ploemen, J. H. T. M., Van Schanke, A., van Ommen, B., & van Bladeren, P. J. (1994b) *Cancer Res. 54*, 915−919.
Puchalski, R. B., & Fahl, W. E. (1990) *Proc. Natl. Acad. Sci. U.S.A. 87*, 2443−2447.
Read, R. J. (1986) *Acta Crystallogr. A42*, 140−149.
Reinemer, P., Dirr, H. W., Ladenstein, R., Huber, R., Lo Bello, M., Federici, G., & Parker, M. W. (1992) *J. Mol. Biol. 227*, 214−226.
Rossmann, M. G., Argos, P. (1975) *J. Biol. Chem. 250*, 7525−7532.
Sinning, I., Kleywegt, G. J., Cowan, S. W., Reinemer, P., Dirr, H. W., Huber, R., Gilliland, G. L., Armstrong, R. N., Ji, X., Board, P. G., Olin, B., Mannervik, B., & Jones, T. A. (1993) *J. Mol. Biol. 232*, 192−212.
Taylor, C. W., Brittain, M. G., & Yeoman, L. C. (1985) *Cancer Res. 45*, 4422−4427.
Teichner, B. A., Holden, S. A., Kelley, M. J., Shea, T. C., Cucchi, C. A., Rosowsky, A., Henner, W. D., & Frei, E. (1987) *Cancer Res. 47*, 388−393.
Tsuchida, S., & Sato, K. (1992) *CRC Crit. Rev. Biochem. Mol. Biol. 27*, 337−384.
Wallace, A. C., Laskowski, R. A., & Thornton, J. M. (1995) *Protein Eng. 8*, 127−134.
Wang, A. L., & Tew, K. D. (1985) *Cancer Treat. Rep. 69*, 677−682.
Waxman, D. J. (1990) *Cancer Res. 50*, 6449−6454.
Wilce, M. C. J., & Parker, M. W. (1994) *Biochim. Biophys. Acta 1205*, 1−18.
Yang, W. Z., Begleiter, A., Johnston, J. B., Israels, L. G., & Mowat, M. R. (1992) *Mol. Pharmacol. 41*, 625−630.

BI962316I